



Signatures of Scalar Dark Energy in $t\bar{t} + E_T^{miss}$ events in ATLAS

Áron Csaba Bodor, Eötvös Loránd University, Budapest, Hungary

September 6, 2017

Abstract

Here put a short abstract of what one can find in this document

Contents

1	Introduction	3
1.1	Dark energy	3
1.2	Connection to particle physics	3
2	Theory	3
2.1	Signals	3
3	Analysis	4
3.1	Aims and strategy	4
3.2	Processing signals	5
3.2.1	Applying the cuts to truth level signals	7
3.2.2	Preselection	7
3.2.3	Optimised selection for each signal region	8
3.2.4	Efficiencies	9
3.3	Results	12
3.4	Conclusion and future plans	15

1 Introduction

1.1 Dark energy

Here comes some general stuff about dark energy and cosmology.

1.2 Connection to particle physics

Here comes the discrepancy between the SM and DE. Is there any reason to think about Dark Energy in a particle viewpoint?

2 Theory

1.5 pages at the least.

Here comes some stuff about the theory we use in general (including some EFT stuff), the parameter M , and linear coefficients C_i .

2.1 Signals

Here comes the derivation of the two operators we try to observe, or put constraints on, and how they scale, what does that mean, how could we observe them.

→ 0L channel

3 Analysis

3.1 Aims and strategy

The aim of my project was twofold: investigate whether signal regions from previous analyses are usable for the search of the specified dark energy signal and if so, to put stricter constraints on the model's M parameter by exclusion. To do this I obtained signal samples of the model. These samples were on truth (or particle) level as reconstructed ones were not yet generated. The signal regions were from previous dark matter and supersymmetry searches, namely [2, 3]. The corresponding truth level signal samples used as benchmark for these regions were made available for me and the expected number of background events (on reconstructed level, both before and after fitting) was accessible in the internal notes. These resources proved enough for a truth level study on the dark energy model.

The mentioned dark matter signal regions were optimised to the processes of dark matter pair production via a scalar mediator, Φ . The process is parametrised by the mass of the mediator, m_Φ . The graph of this process could be seen on Figure 1.

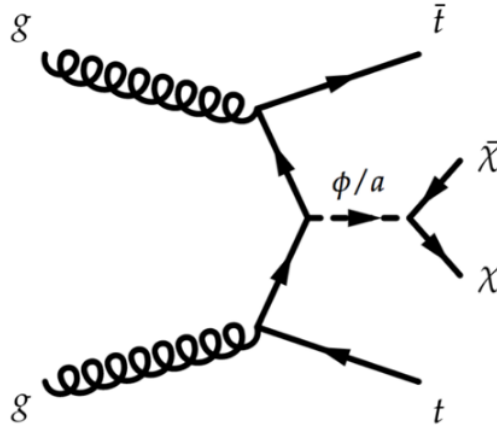
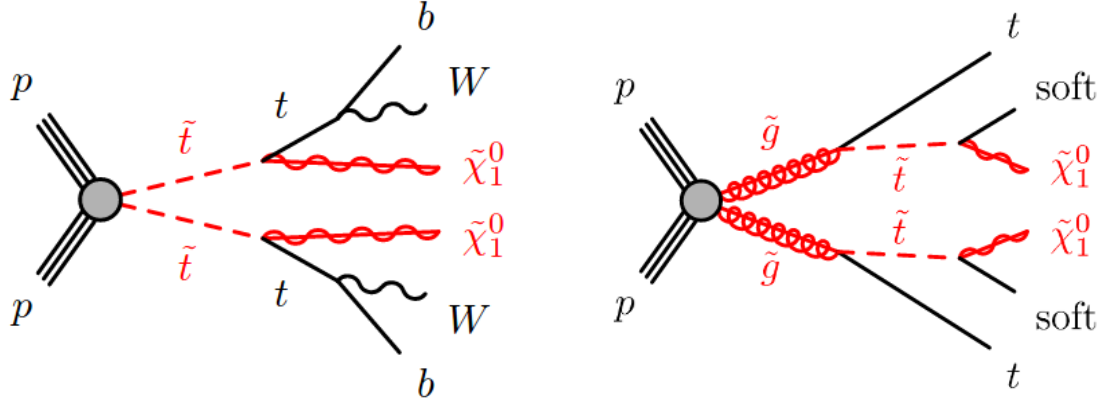


Figure 1: Feynman diagram for the dark matter pair production process via a scalar mediator.

In the case of supersymmetry two schemes were considered: a process in which stop-pairs produced directly and one in which they are from the decay of gluinos (gluino mediated stop production). These processes are governed by the supersymmetric particle masses, namely $m_{\tilde{g}}$, $m_{\tilde{t}}$ $m_{\tilde{\chi}}$. Figure 2 show the graphs of these processes.



(a) Direct stop production

(b) Gluino mediated stop production

Figure 2: Feynman graph of supersymmetry processes used to develop the signal regions.

3.2 Processing signals

The signal regions used were 'HIGH' and 'LOW' from the dark matter analysis [2], and 'A', 'B', 'E' from the supersymmetry investigation [3]. In table 1 the relevant physical parameters of the signals used to optimise the region are listed.

Before starting the detailed analysis it is advised to have a look at the E_T^{miss} distributions of the processes. Comparing the generated DE signals to DM on Figure 3 we can see that the DE signal has a harder E_T^{miss} spectrum. We can also see, that due to cuts in this variable (typically $E_T^{miss} > 300$ GeV) the resulting DMLOW yield from the according benchmark signal will be low. The kink in the DMLOW reference spectrum at around 60 GeV is due to the skimming filter applied to the sample.

We can also see that the SUSY signals have harder spectrum averaging in all cases above the DM ones. The SRA and SRE reference signal averages above the DE signal, but not the SRB. We will see that this is correlates to the yields after cuts.

Signal region name	Benchmark sample parameters
DMLOW	$m_\Phi = 20$ GeV
DMHIGH	$m_\Phi = 300$ GeV
SRA	$m_{\tilde{t}} = 1$ TeV, $m_{\tilde{\chi}} = 1$ GeV
SRB	$m_{\tilde{t}} = 600$ GeV, $m_{\tilde{\chi}} = 300$ GeV
SRE	$m_{\tilde{g}} = 1.7$ TeV, $m_{\tilde{t}} = 400$ GeV

Table 1: Physical parametrisation of the benchmark samples.

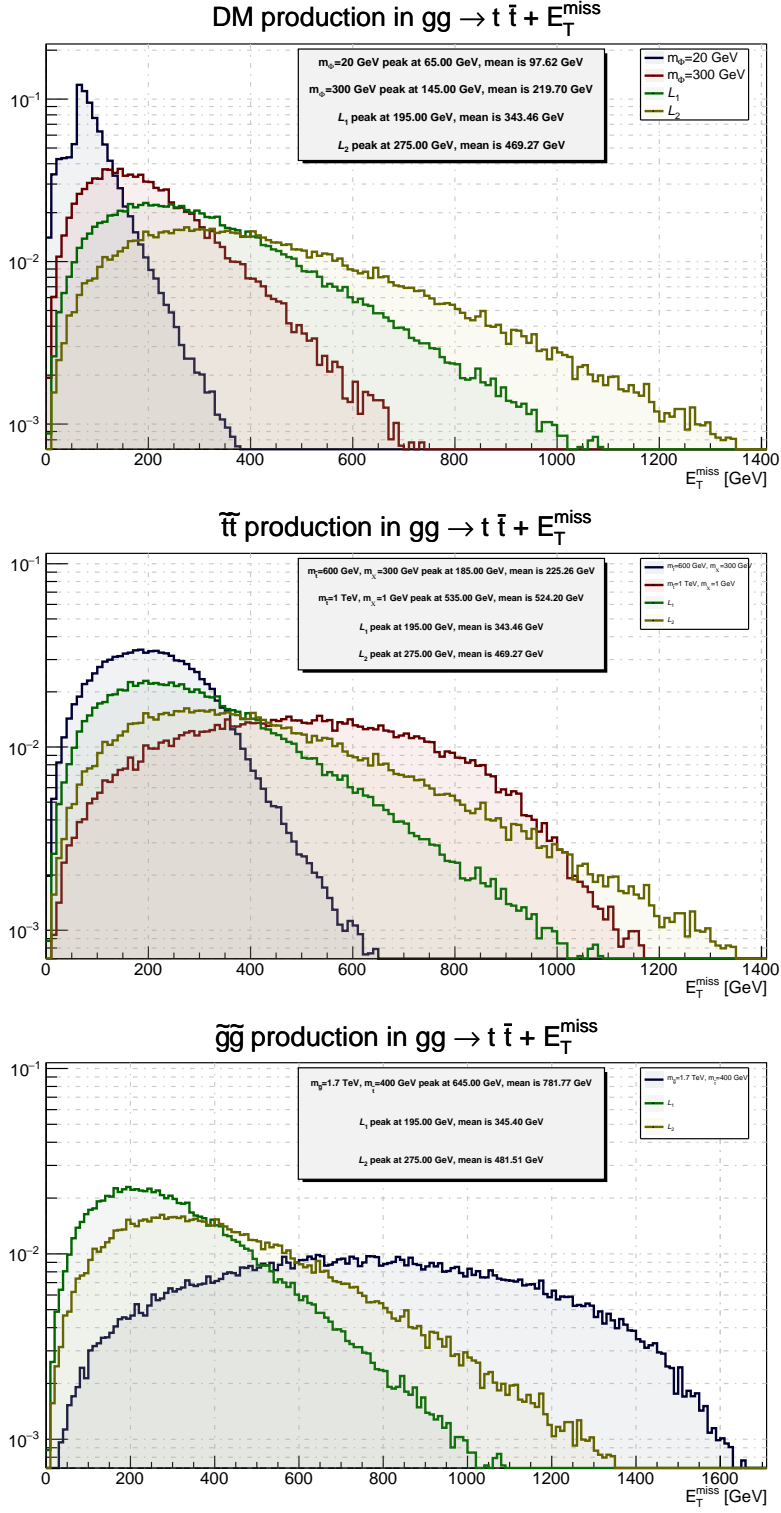


Figure 3: Missing transverse energy spectra of the reference signals (blue, red) compared to the DE signals (green, yellow).

3.2.1 Applying the cuts to truth level signals

The cuts prescribed in [2, 3] are developed using reconstructed samples. Issues arise if one tries to apply them directly to truth level samples, because in some cases the required variable in which the cut is made is not defined at truth level. During the analysis two of these issues were addressed, one of which concerns the τ -veto, see that later.

The other problem considered is connected to the b -jettagging efficiency. As on truth level we don't have the MV2c10 b -tagging discriminant, all of them considered tagged with 100% efficiency. However the cuts require a 77% tagging efficiency, so we addressed the issue with random generating numbers for all b -jets from a uniform distribution on $[0, 1]$. Those with scores below 0.77 remain a b -jet, the others are not considered as b -jets any more. This implies that all b -jetconnected variables (e.g. $m_T^{b, min}$) has to be recalculated during this process.

3.2.2 Preselection

The DM and SUSY analyses both define similar preselection cuts to insure that we are defining signal regions in the correct decay channels and to improve purity. Aiming to capture the correct decay channel we apply:

- lepton-veto (electrons, muons),
- number of jets at least four with $p_T > [80, 80, 40, 40]$ GeV,
- number of b -jets at least two,
- τ (-jet) veto (except for SRE).

These cuts comes trivially seeing the decay scheme. As it was pointed out in the previous subsection some issues arise with the last cut, as it requires the reconstructed variable $E_T^{miss, track}$, the missing transverse energy measured by the tracker. To circumvent these a truth level τ - jet overlap removal was applied the following way:

1. select the non- b -jet closest to E_T^{miss} with $|\Delta\Phi(E_T^{miss}, \text{jet})| < \pi/5$,
2. scan truth level τ particles, reject event if $\Delta R(\text{truth } \tau, \text{selected jet}) < 0.2$.

To reduce the background and reject fake events from mismeasured jet p_T :

- $E_T^{miss} > 300$ GeV (DM), 250 GeV (SUSY),
- $|\Delta\Phi(p_T, E_T^{miss})| > 0.4$ for the leading 4 (DM) or 3 (SUSY) jets.

3.2.3 Optimised selection for each signal region

To maximise the expected sensitivity more detailed cuts are applied, this time these are different for all signal regions. The discriminating variables used to make these cuts:

- m_{AkT8} , m_{AkT12} : reclustered jet masses with anti- k_T parameters $R = 0.8$ and $R = 1.2$; cuts in these variables ensure that we select events with W -boson and top-quark involved,
- $m_T^{b, min}$, $m_T^{b, max}$: transverse mass of the b -jet lying closest and furthest to E_T^{miss} ; these variables provide good discrimination to the semileptonic $t\bar{t}$ -background.
- H_T : scalar sum of the jet transverse momenta,
- $E_T^{miss}/\sqrt{H_T}$: missing transverse energy significance,
- $\Delta R(b, b)$: the distance of the two b -jets with highest MV2c10 scores; discriminates against the $Z + b$ -jets background, where the b -jets arise from gluon-splitting,
- m_{T2} : also known as stransverse momentum.

The concrete cuts for each region are listed in Table 2. As mentioned in 3.2.1 every b -jetrelated variable had to be recalculated during the analysis. This could be carried unambiguously for all variables of this kind, except for $\Delta R(b, b)$. As we have no proper discrimination on which two b -jets to use, all possible combinations were calculated and the smallest ΔR was chosen.

Cut	DMLOW	DMHIGH	SRA	SRB	SRE
m_{AkT8}^0	>80	-	>60	-	>120
m_{AkT8}^1	>80	-	-	-	>80
m_{AkT12}^0	-	>140	>120	>120	-
m_{AkT12}^1	-	>80	>120	>120	-
$m_T^{b, min}$	>150	>200	>200	>200	>200
$m_T^{b, max}$	>250	-	-	>200	-
m_{T2}	-	-	>400	-	-
H_T	-	-	-	-	>800
$E_T^{miss} \sqrt{H_T} [\sqrt{\text{GeV}}]$	-	>12	-	-	>18
E_T^{miss}	-	-	>400	-	>550
$\Delta R(b, b)$	>1.5	>1.5	-	>1.2	-

Table 2: Cuts specified for each investigated signal region. All variables are understood in GeV, except for the missing transverse energy significance, where units are shown explicitly.

3.2.4 Efficiencies

After applying the cuts, the efficiencies could be calculated for all samples and regions:

$$\text{Efficiency} = \frac{\# \text{ events after cuts}}{\# \text{ events before cuts}}. \quad (1)$$

Evaluating (1) after each cut results in the cutflows. Plotting these can show which cut made the most difference to a signal sample. Cutflow plots are also a suitable tool to compare different signals in the same region. Figures 4 to 8 show these plots. Referring back to the introduction of section 3.2 it is apparent that whichever signal has the harder E_T^{miss} spectrum will dominate in terms of efficiency after the cuts. This correlates with the fact that the cuts in E_T^{miss} made the most change in the efficiencies (not considering the necessary cuts of the decay channel). The numerical values in form of percentages of the efficiencies can be found in Table 3.

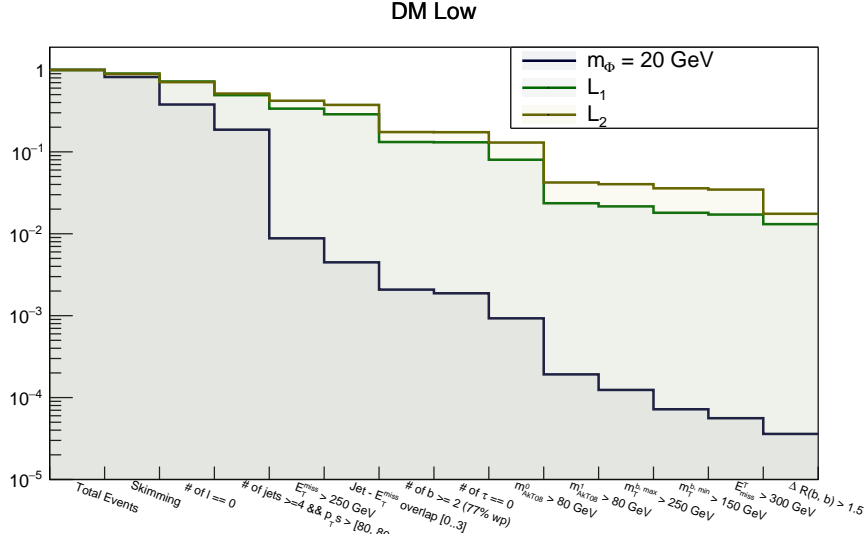
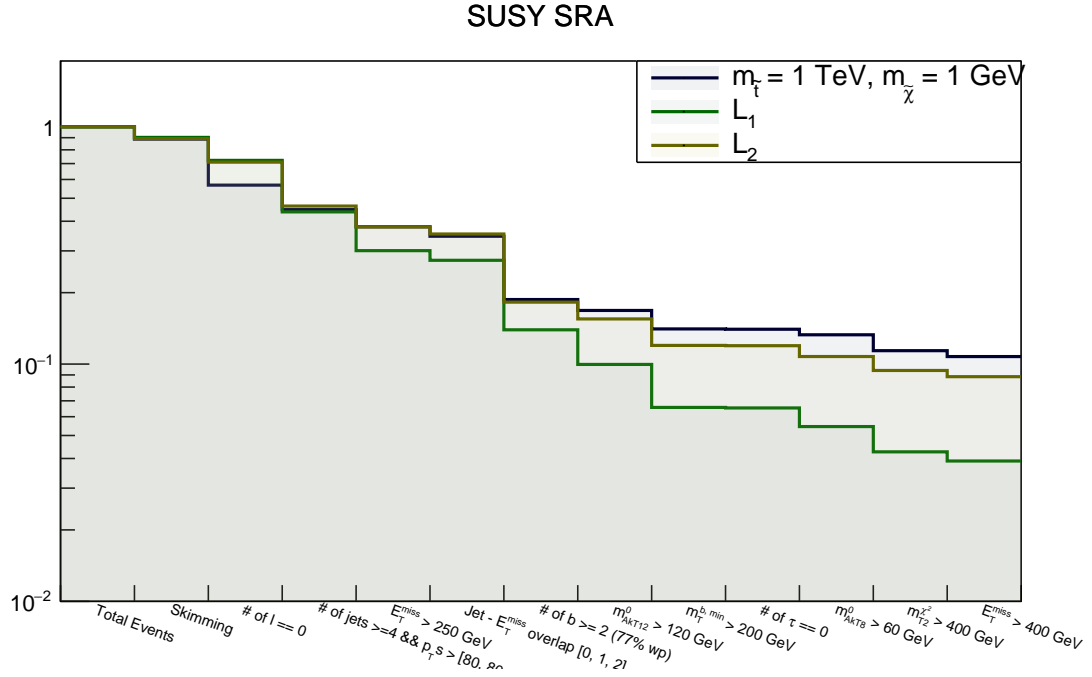
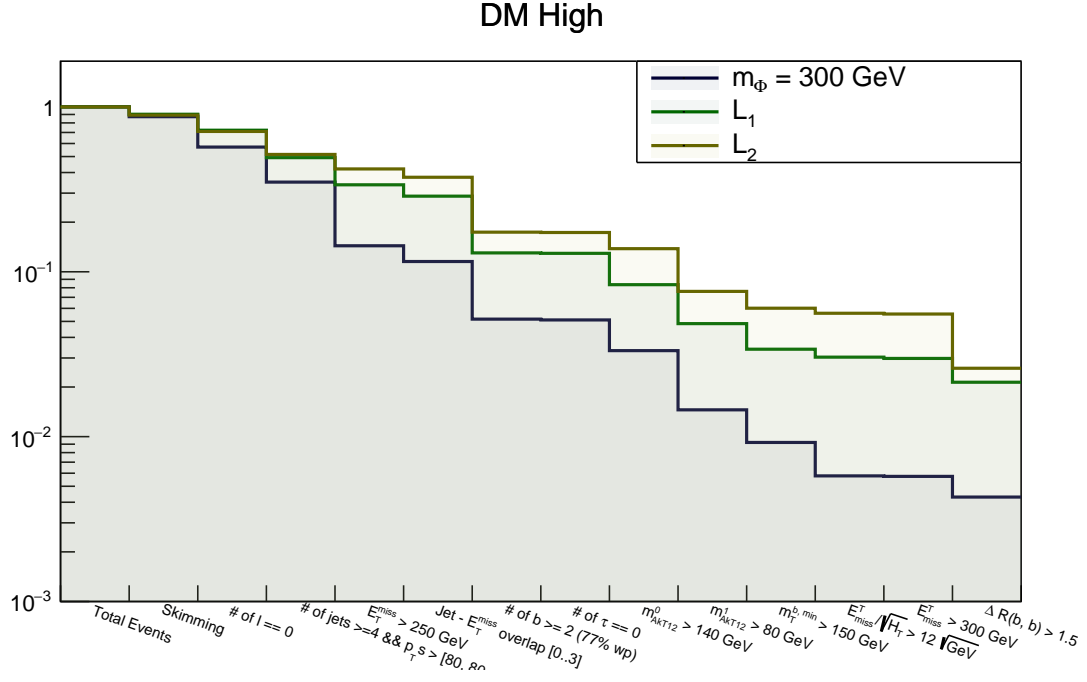


Figure 4: Cutflow plot of the signal region DMLOW.

Signal region	Reference	\mathcal{L}_1	\mathcal{L}_2
DMLOW	0.0036 %	1.31 %	1.75 %
DMHIGH	0.43 %	2.14 %	2.60 %
SRA	10.76 %	3.90 %	8.85 %
SRB	1.48 %	5.22 %	6.90 %
SRE	7.00 %	0.56 %	1.63 %

Table 3: Efficiencies of DE samples compared to the benchmark samples.



SUSY SRB

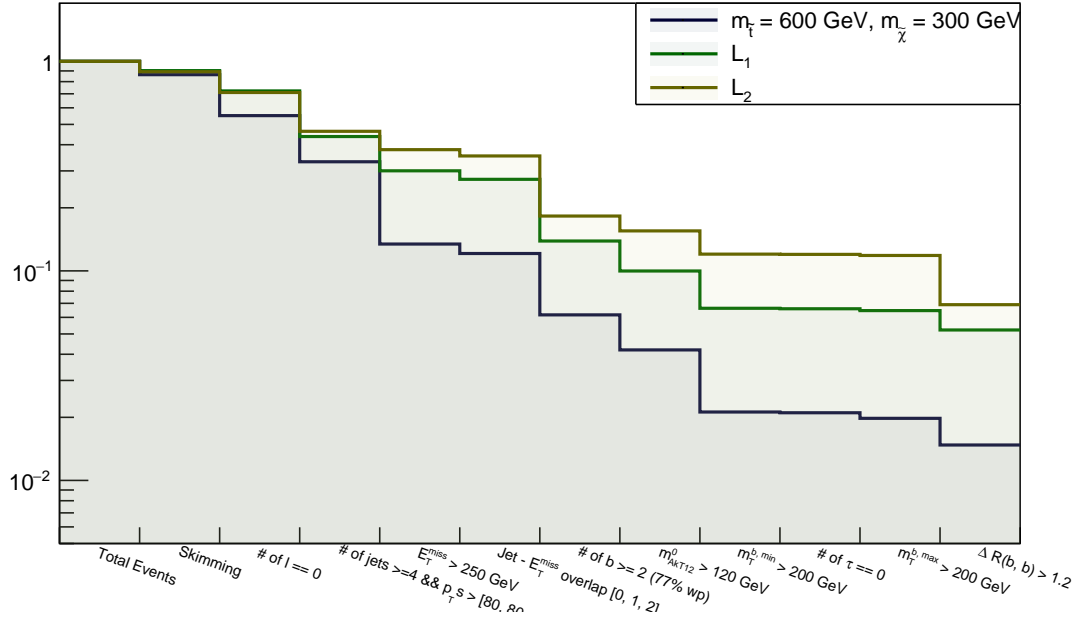


Figure 7: Cutflow plot of the signal region SRB.

SUSY SRE

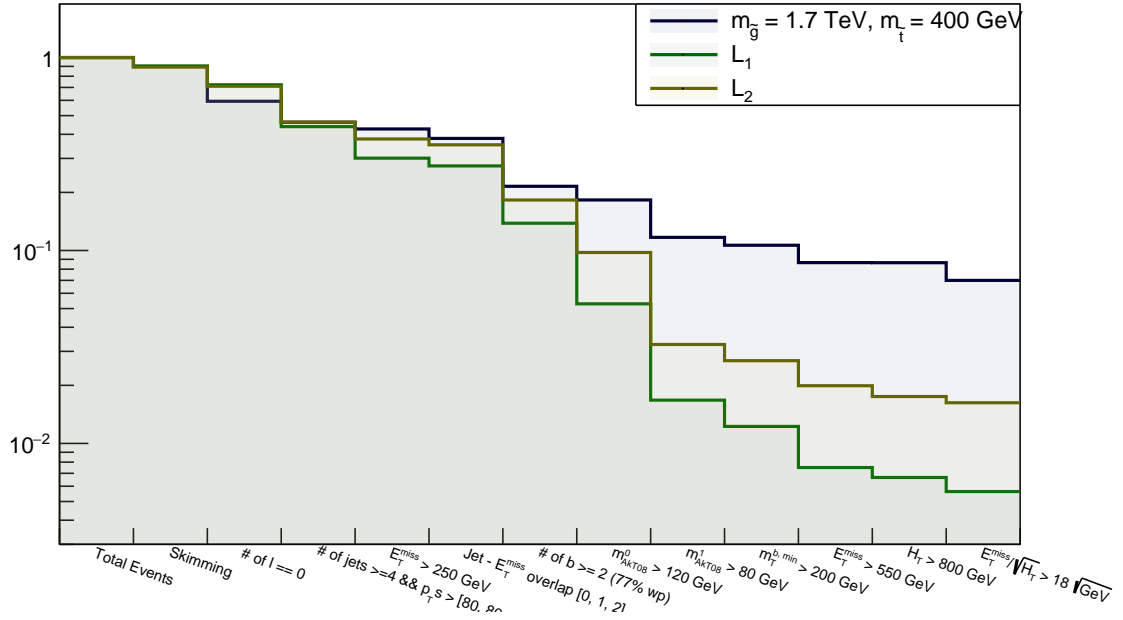


Figure 8: Cutflow plot of the signal region SRE.

3.3 Results

Using the results from Subsection 3.2 we can calculate the yields for arbitrary luminosity.

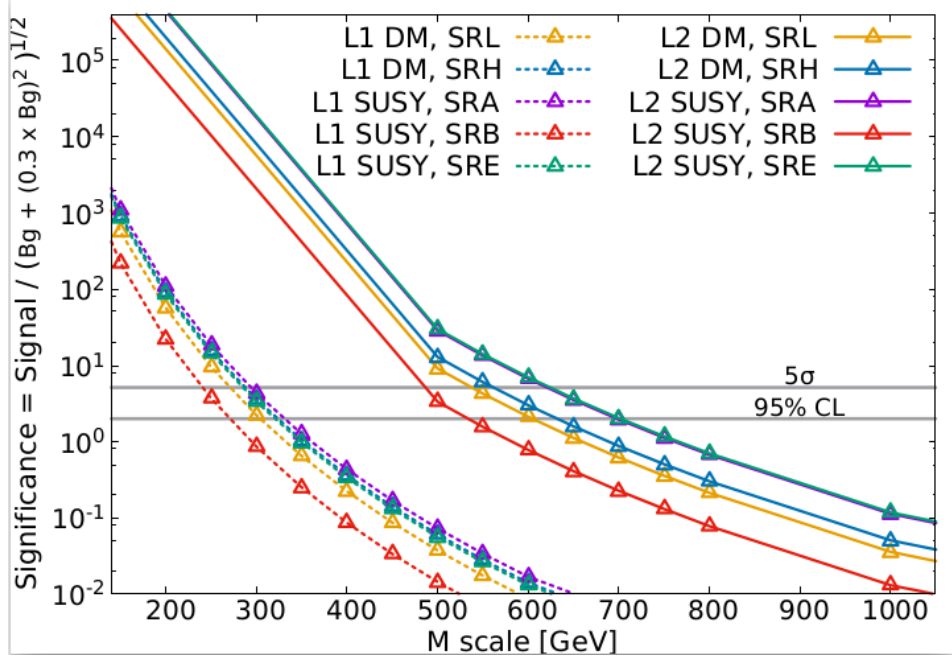


Figure 9: Significances on truth level. It apparent that we can be sensitive to \mathcal{L}_2 to higher scale than to \mathcal{L}_1 , but monojet analyses expected to be more significant to \mathcal{L}_2 than $t\bar{t}$ analyses.

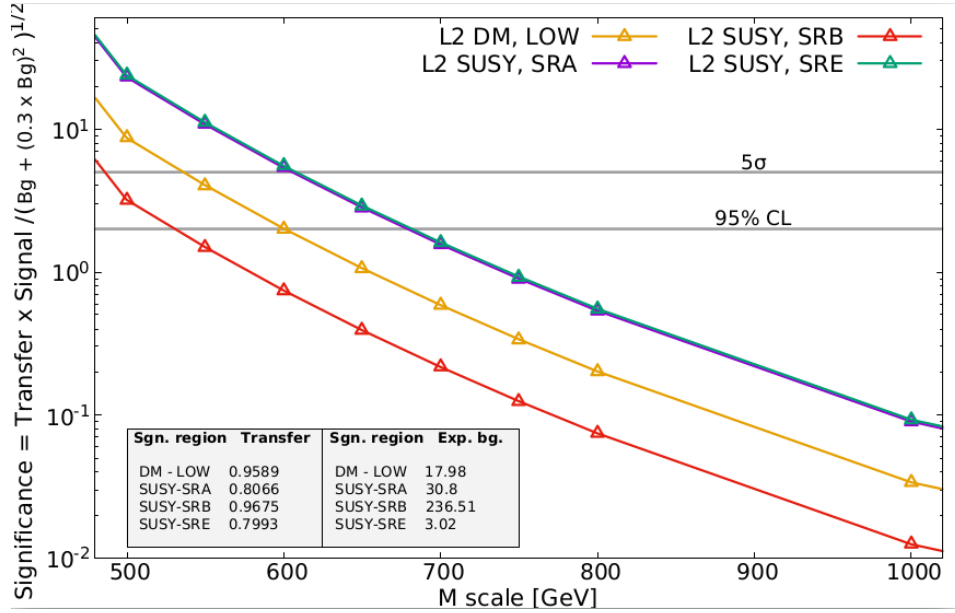


Figure 10: Significances involving the \mathcal{L}_2 operator extrapolated to reconstructed level, see (??).

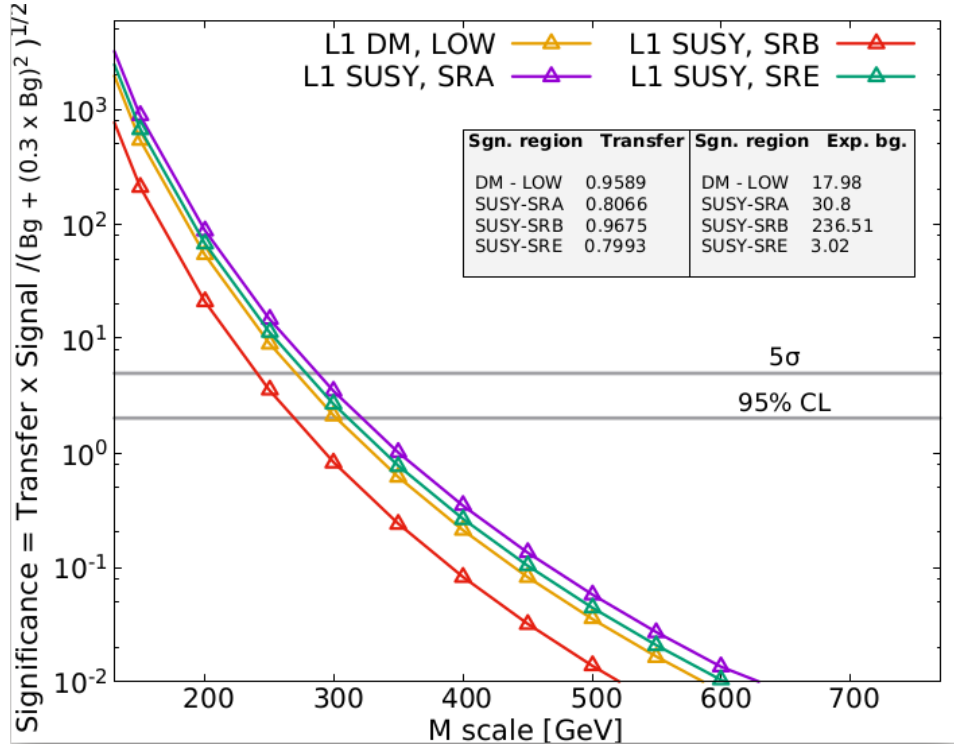


Figure 11: Significances involving the \mathcal{L}_1 operator extrapolated to reconstructed level. It is apparent that we can expect better exclusion limits with a detailed analysis than [1] according to this naive extrapolation.

3.4 Conclusion and future plans

References

- [1] Study of ... *Author name*